Use of a Diels-Alder reaction to modify thermal expansion properties in charge-transfer cocrystals

Journal:	*CrystEngComm*
Manuscript ID	CE-COM-09-2022-001207
Article Type:	Communication
Date Submitted by the Author:	01-Sep-2022
Complete List of Authors:	George III, Gary; Texas Tech University, Chemistry & Biochemistry Unruh, Daniel; Texas Tech University, Chemistry and Biochemistry Hutchins, Kristin; Texas Tech University, Chemistry & Biochemistry

COMMUNICATION

Use of a Diels-Alder reaction to modify thermal expansion properties in charge-transfer cocrystals

Gary C. George III, Daniel K. Unruh and Kristin M. Hutchins*

A strategy for modifying thermal expansion properties in dichroic, charge-transfer cocrystals is described. A solid-state Diels-Alder reaction is used to covalently connect adjacent molecules in the cocrystal, and thermal expansion along the direction of these bonds is reduced when compared to the unreacted cocrystals.

The ability to control the thermal expansion (TE) behaviors of materials is of high interest within chemistry, materials science, and engineering.[1] Understanding and controlling how a material responds to temperature changes (i.e., TE) is important,[2] especially for materials used in applications where thermal changes occur.[3] The molecular structure of the component(s) and the way in which components are connected in three dimensions has an impact on how a material responds to temperature changes.[4] For organic solid materials, the TE is often dictated by the strength of the noncovalent interactions holding neighboring molecules together.[5] Work by our group and others has focused on using noncovalent interactions such as hydrogen and halogen bonds to control TE within organic solids.[6] Some work has focused on cocrystals, which are solids containing two or more molecular components in a fixed stoichiometric ratio.[7] Inclusion of multiple components in the crystal lattice can also lead to useful properties such as reactivity, enhanced solubility, and unique optical properties.[8]

In the area of reactivity, our group demonstrated that a solid-state [2+2] cycloaddition reaction altered TE behavior in a cocrystal.[9] Specifically, the TE was halved along the direction where covalent bonds formed after the cycloaddition. This initial observation led us to a hypothesis; replacement of noncovalent interactions with covalent bonds will increase the strength along a given direction and, therefore, decrease TE.

To test this hypothesis, we chose to investigate a charge-transfer cocrystal system containing bis(N-allylimino)-1,4-dithiin (DA2) and 9-bromoanthracene (BrAn) because the cocrystal has been reported to undergo a single-crystal-to-crystal Diels-Alder reaction in the solid state.[10] The reported reactive cocrystal has the nearest BrAn molecules arranged head-to-tail (H-T) within the π stack, meaning that every other BrAn molecule is rotated by 180° (Scheme 1a). The authors mention that a second crystal of different morphology was observed in the crystallization vial containing DA2 and BrAn, but was unable to be characterized.
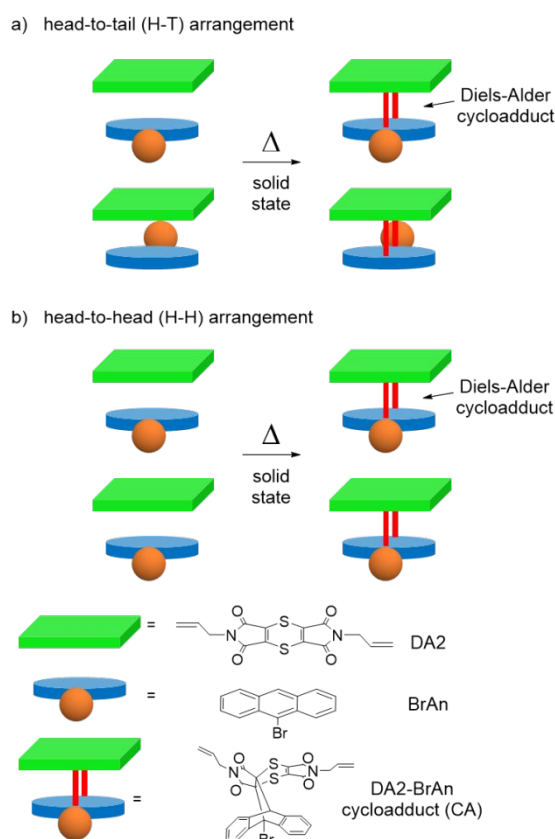
Scheme 1. Charge-transfer cocrystal polymorphs containing DA2 and BrAn arranged in a (a) H-T or (b) H-H geometry to undergo a Diels-Alder cycloaddition in the solid state.

Department of Chemistry and Biochemistry, Texas Tech University, Lubbock, TX, 79409 USA. Email: kristin.hutchins@ttu.edu

Here, we demonstrate that TE of organic solids can be modified by forming covalent bonds via a Diels-Alder cycloaddition. We show that although the overall TE in the solids before and after reaction is comparable, the directions of highest TE switch following the reaction, and less TE occurs along the direction where newly formed covalent bonds lie. In addition to conducting a variable-temperature solid-state behavior analysis of the previously published H-T DA2-BrAn cocrystal, we successfully determined the structure for the second charge-transfer cocrystal that forms concomitantly. The second cocrystal is a polymorph, and the nearest BrAn molecules are arranged head-to-head (H-H) within the π stack (Scheme 1b). We show that the H-H DA2-BrA cocrystal also undergoes a Diels-Alder reaction in the solid state upon heating at 90-100 °C for one week. Interestingly, the H-T cocrystal reacts in the solid state at ca. 40 °C for a period of one month, but the H-H cocrystal is unreactive at the same temperature. Thus, cocrystallization of DA2 and BrAn affords two reactive polymorphs that require different temperatures to undergo a solid-state Diels-Alder cycloaddition. To the best of our knowledge, this is the first report using Diels-Alder reactions to modify TE properties of organic materials.

DA2 was synthesized using the previously reported method (Figure S5-S6).[10] The previous report obtained concomitant cocrystallization of plate- and needle-shaped crystals using vapor diffusion of hexane into dichloromethane (DCM), and X-ray data was collected for crystals with the plate morphology.

We used vapor diffusion or slow evaporation to isolate cocrystals of the two DA2-BrAn polymorphs. Vapor diffusion of hexanes into a DCM solution containing a 1:1 molar ratio of DA2 and BrAn resulted in a larger amount of the H-T polymorph (plates), while giving concomitant crystallization of the H-H polymorph. On the other hand, slow evaporation of a DCM solution containing a 1:1 molar ratio of DA2 and BrAn afforded primarily the H-H polymorph (needles), but there was still concomitant crystallization of the H-T polymorph.

The two charge-transfer polymorphs containing DA2 and BrAn are distinguishable by polarized optical imaging. The H-T polymorph exhibits orange to green dichroism and crystallizes as large plates, whereas the H-H polymorph is only orange, and crystallizes as thin, elongated plates (Figure 1). The use of vapor diffusion and slow evaporation methods afforded differing amounts of the two polymorphs in solution. Powder X-ray diffraction (PXRD) demonstrated that the bulk material obtained from vapor diffusion contained approximately 80% of the H-T polymorph and 20% of the H-H polymorph (Figure S16). On the other hand, use of slow evaporation afforded approximately 13% of the H-T polymorph and 87% of the H-H polymorph as evidenced by PXRD characterization of the bulk material (Figure S17). ^{1}H NMR spectra of the concomitantly obtained DA2-BrAn cocrystals demonstrated that the components were present in a 1:1 ratio (Figure S7).

The components within the H-T cocrystal crystallized in the monoclinic space group, $P2_1/n$, whereas the components in the H-H cocrystal crystallized in the triclinic space group, $P-1$. Both cocrystals contain one molecule of DA2 and one molecule of BrAn in the asymmetric unit. Both solids consist of infinite π-
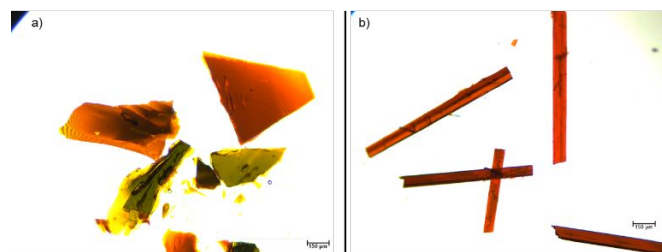

Figure 1. Polarized light microscopy images of the two DA2-BrAn polymorphs: a) large dichroic plates of the H-T polymorph and b) thin, elongated plates of the H-H polymorph.

stacks of alternating DA2 and BrAn molecules. As shown in Scheme 1, H-T and H-H refer to the location of the bromine atom on the BrAn molecule within the stacks (Figure 2). The position of the allyl groups on DA2 also differs in the polymorphs. The allyl groups of DA2 in the H-T polymorph alternate so that from one DA2 to another within the π-stack, they are oriented *trans* to each other, whereas in the H-H polymorph, the allyl groups in one DA2 are *cis* to the next DA2 molecule in the π-stack. The packing between neighboring π-stacks also differs between the two polymorphs (Figure S22-S23). In the H-T polymorph, neighboring π-stacks are close packed and the BrAn molecules lie in the same orientation between the stacks. In the H-H polymorph, neighboring π-stacks are arranged pairwise, where the stacks within each pair lie close packed to each other. Each pair is separated by a longer distance, and the BrAn molecules are rotated by 180° between neighboring π-stacks.

Solid-state cycloaddition reactions were conducted by placing vials that contained both polymorphs (due to concomitant crystallization) in an oven at 40-50 °C for approximately one month. These conditions afforded a Diels-Alder reaction for the previously described H-T polymorph.[10] The H-T polymorph undergoes a Diels-Alder reaction in the solid state at room temperature, but heating accelerates the reaction. Upon reaction, the H-T polymorph showed enhanced mosaicity by viewing under an optical microscope (Figure S12), along with a color change from the orange-green dichroism to an opaque yellow, and the absence of meaningful diffraction peaks in a SCXRD experiment. Under the same experimental conditions, the H-H polymorph showed no sign of reaction as the crystals retained crystallinity and complete diffraction capabilities even after extended periods of time in the oven. SCXRD data collected on the H-H polymorph after one month of heating also demonstrated that no reaction had taken place. Thus, the reaction temperature was increased to determine if reactivity was possible for the H-H polymorph. Crystals of the H-H polymorph were heated in an oven at 90-100 °C for a period of one week, which resulted in enhanced mosaicity as evidenced by optical microscopy (Figure S13), absence of meaningful diffraction peaks in a SCXRD experiment, and a change in color from orange to opaque yellow.
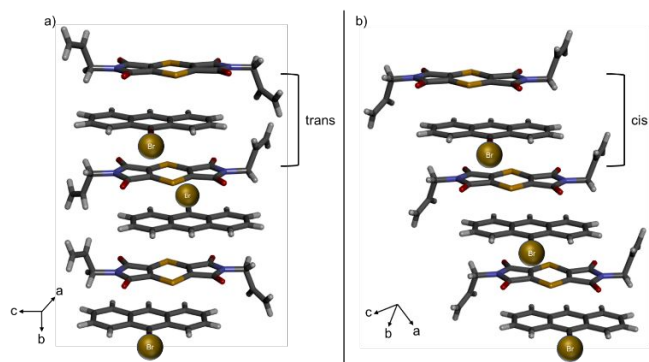
COMMUNICATION

Figure 2. X-ray crystal structures of DA2-BrAn polymorphs: (a) H-T and (b) H-H highlighting π-stacking arrangement and positions of the bromine atoms and allyl groups.

Following cycloadditions, the products were recrystallized to obtain high-quality single crystals, and two unique products were isolated, in accordance with the previous report. Slow evaporation of the reacted H-T material from DCM afforded a DCM solvate of the cycloadduct (CA). The previous report also obtained the non-solvated CA of the H-T product from DCM. Here, we obtained the non-solvated CA via slow evaporation from chloroform. The reacted solid of the H-H polymorph was also recrystallized from DCM and chloroform. Both experiments afforded single crystals that were isostructural to the H-T cycloadducts (solvate with DCM and non-solvate, Table S13). The SCXRD data confirmed that the solid-state Diels-Alder reactions were successful for both the H-T and H-H polymorphs, as the DA2 and BrAn molecules are connected through covalent bonds in the structure. Unfortunately, we were not able to conduct the cycloadditions in a single-crystal-to-single-crystal fashion, which would result in distinct crystal structures due to the arrangement of bromine atoms in the extended structure.

^{1}H NMR spectra of the non-solvated CA and DCM solvate of the CA showed significant upfield shifts for the aromatic hydrogens on BrAn (Figure S8-S9). The hydrogen in the center of the BrAn component also shifts upfield significantly due to the change in carbon hybridization from sp^2 to sp^3. The DA2 component also becomes unsymmetrical following the Diels-Alder reaction, which is evidenced in the NMR spectra. A total of six signals for the hydrogens on the allyl groups are present (instead of three) in the non-solvate and DCM solvate of the CAs. A small amount of unreacted material is also present in the NMR spectra of the CAs.

The non-solvated CA crystallized in the *P2₁/c* space group and contains one CA molecule in the asymmetric unit. Upon expanding the structure, neighboring CAs are oriented perpendicular to each other (Figure 3a). The CAs stack into columns that extend approximately along the *ab* plane. Within the column, the CA molecules stack in an AABB pattern, wherein A is a CA with the covalent linkage oriented vertically and B is a CA with the covalent linkage oriented horizontally. The non-solvated CAs interact through a combination of weak interactions including C-H···O, O···N, C-H(allyl)··· π(allyl), S···S, C-H···Br, Br···O, and C-H···π.

The solvated CA crystallized in the *P-1* space group and contains one molecule of the CA and one molecule of DCM in the asymmetric unit. The CAs within the DCM solvate are arranged in infinite parallel stacks, with all the newly formed covalent bonds lying in the same direction (Figure 3b). The solvated CAs interact through a combination of weak interactions including C-H···O, O···S, S···S, C-H···S, and C-H···π. The DCM solvent molecules interact with the CA units via C-H···O, C-H···π, and Cl···O interactions. A SCXRD experiment was performed for a single crystal of the DCM solvate of the CA after solvent had been lost from the crystal lattice; however, the crystal was highly mosaic and failed to produce any meaningful diffraction peaks.
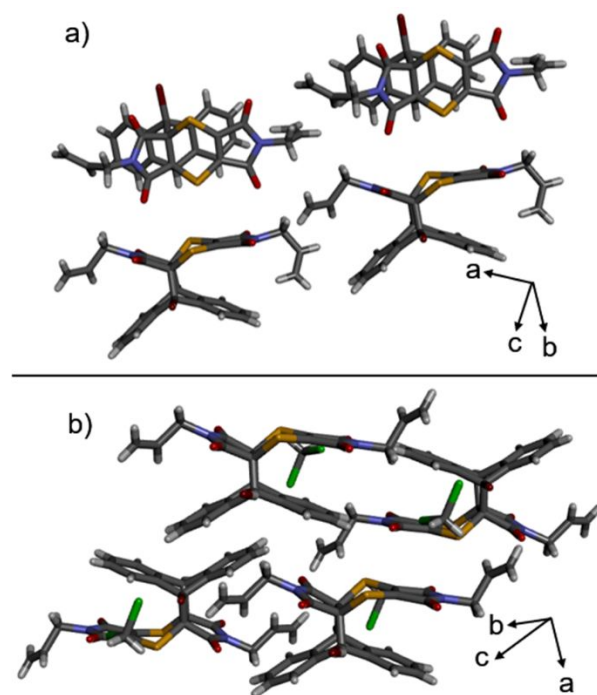

Figure 3. X-ray crystal structures of the CAs: a) non-solvated and b) DCM solvate.

Table 1. TE coefficients for the crystals. Errors are denoted in parentheses and approximate crystallographic axes are denoted in brackets.

| Crystal	α_{X_1} (MK⁻¹) [axis]	α_{X_2} (MK⁻¹) [axis]	α_{X_3} (MK⁻¹) [axis]	α_V(MK⁻¹)
DA2-BrAn H-T	8 (1) [3 0 -1]	56 (2) [3 0 4]	113 (3) [0 1 0]	179 (5)
DA2-BrAn H-H	17 (1) [2 5 -1]	38 (1) [-4 1 2]	130 (3) [5 -1 2]	188 (3)
DA2-BrAn CA non-solvated	28 (3) [1 0 -5]	47 (1) [0 -1 0]	90 (8) [4 0 3]	168 (6)
DA2-BrAn CA solvate	16 (1) [-1 1 1]	58 (2) [1 1 0]	109 (3) [4 -1 3]	186 (5)

A variable temperature X-ray diffraction experiment was conducted for both DA2-BrAn cocrystal polymorphs, as well as the solvated and non-solvated CAs. Each crystal was mounted at 100 K and warmed to 300 K while collecting data sets every 20 K. A total of 11 full X-ray data sets were conducted for all four crystals. PASCal[11] was used to calculate the three principal axes

COMMUNICATION   **Journal Name**

of TE (X_1, X_2, and X_3), the three linear TE coefficients (α_{X1}, α_{X2}, and α_{X3}), and the volumetric TE coefficient (α_V) using the variable temperature X-ray data (Table 1). Variable-temperature optical microscopy was also conducted for each crystal before and after the solid-state Diels-Alder reaction to assess dimensional changes between the original cocrystal and pre-recrystallized cycloadduct (Figure S24-25).

The TE properties for both DA2-BrAn cocrystals (H-T and H-H) are dominated by C-H⋯O interactions in the X_1 direction, with the average C-H⋯O distance change of 0.056 and 0.075 Å, respectively, and C-H⋯O, C-H⋯π, and C-H⋯S contacts in the X_2 direction. The TE of the H-T and H-H forms are dominated primarily by π-π stacking in the X_3 direction, with an average π-π stacking distance change of 0.082 and 0.084 Å, respectively. The intermolecular interaction length changes are provided in Table S15. In the H-T cocrystal, the least and median expansion (α_{X1} and α_{X2}) occurs between the neighboring π stacks of DA2 and BrAn molecules in nearly perpendicular directions. The X_1 axis lies along the short length of the molecules and the direction of the bromine atoms, while X_2 is along the longer length of the molecule and in the direction of the allyl groups (Figure 4a, Table 1). The most expansion, α_{X3}, within the DA2-BrAn H-T cocrystal occurs along the π-stacking direction. This is also the direction in which the new covalent bonds will form during the Diels-Alder reaction.

For the DA2-BrAn H-H cocrystal, the least expansion (α_{X1}) occurs in a similar direction as the H-T polymorph, but the plane is shifted slightly from being completely vertical (Figure 4b). The median expansion (α_{X2}) also occurs in a similar direction as the H-T polymorph, but again the plane is shifted from vertical and includes some contribution from the π-stacking direction. The most expansion (α_{X3}) occurs along the π-stacking direction, but the plane does not lie perfectly horizontal as in the H-T polymorph. Many organic materials exhibit positive TE (PTE),[1g, 2a] and expansion coefficients range from small to moderate to colossal, with colossal corresponding to a TE coefficient above 100 MK^{-1}.[1d] Both DA2-BrAn cocrystals undergo slight PTE along X_1, moderate PTE in X_2, and colossal PTE along X_3 and volumetrically. Overall, the most TE in both unreacted DA2-BrAn cocrystals occurs along the π-stacked direction.

Figure 4. Crystal structures and the planes in which TE occurs perpendicular to for: a) DA2-BrAn H-T polymorph, b) DA2-BrAn H-H polymorph, c) non-solvated CA, and d) DCM solvate of CA (solvent removed for clarity). The TE planes are shown with X_1 in green, X_2 in blue, and X_3 in red.
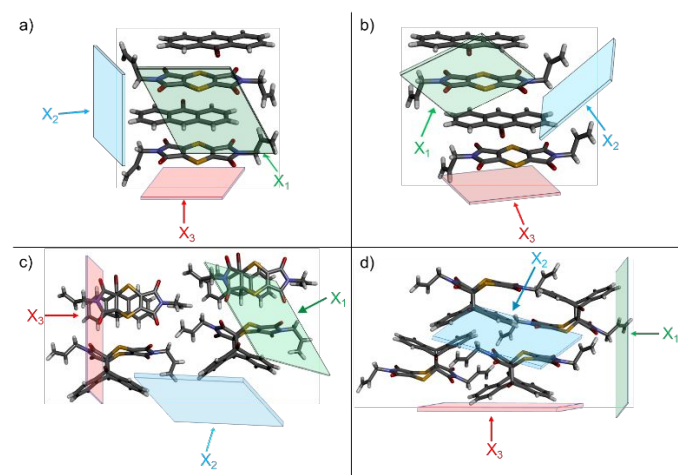
The TE behavior of both CAs is also dominated by C-H⋯O interactions in the X_1 direction with an average C-H⋯O distance change of 0.081 Å for the non-solvated CA and 0.099 Å for the solvated CA. A variety of interactions contribute to expansion along X_2, including S⋯O and C-H⋯π interactions, and X_3 consists of S⋯S, O⋯N, and C-H⋯π interactions. Both CAs lack any significant form of π-π stacking. Both CAs show slight PTE along X_1, moderate PTE along X_2, and colossal or near-colossal PTE in X_3, with colossal positive volumetric coefficients. Thus, when examining the TE coefficient values, the overall behavior does not initially appear to be affected by the Diels-Alder reaction.

However, to compare how the new covalent bonds affect TE, the directions of TE within the structure before and after reaction must be compared. In the unreacted DA2-BrAn H-T and H-H cocrystals, the expansion along X_1 and X_2 occurs between the π stacks of DA2-BrAn molecules and encompass interactions between stacks, while X_3 includes the π-stacked direction. The TE along X_3 is colossal PTE in both cocrystal polymorphs (α_{x3} = 113 and 130 MK^{-1} for H-T and H-H, respectively). In the nonsolvated CA, the new covalent bonds linking DA2 and BrAn lie along X_1 and X_2 instead of X_3, and these directions exhibit small to moderate PTE (α_{x1} = 28 MK^{-1} and α_{x2} = 47 MK^{-1}). Overall, TE along the directions where noncovalent bonds changed to covalent bonds was altered from colossal to small/moderate.

In the DCM solvated CA, the X_1 plane lies between stacks of CA molecules. The covalent bonds in the solvated CA structure lie along the X_2 and X_3 directions, which exhibit moderate and colossal PTE (α_{x2} = 58 MK^{-1} and α_{x3} = 109 MK^{-1}). The formation of covalent bonds has reduced TE in the solvate structure because they contribute to X_2; however, X_3 also includes the covalent bonds and still exhibits colossal expansion. The included DCM molecules engage in weak interactions with neighboring CA molecules and lie along X_1 and X_3. These solvent interactions contribute to the larger TE observed along X_3 in the solvate CA when compared to the non-solvate CA.

A new method for modifying TE properties in organic cocrystals by conducting Diels-Alder reactions to covalently connect adjacent molecules was described. Before reaction, cocrystals exhibit large PTE along the π-stacked direction. After reaction and recrystallization of the product, the cycloadducts exhibits less TE along the direction where new covalent bonds lie, which formed through the Diels-Alder reaction. We are currently investigating other systems and techniques as platforms for modifying and controlling TE.

Notes and references

1. (a) S. J. Baxter, A. Schneemann, A. D. Ready, P. Wijeratne, A. P. Wilkinson and N. C. Burtch, *J. Am. Chem. Soc.*, 2019, **141**, 12849-12854; (b) B. Rădulescu, A. M. Mihalache, A. Hrițuc, M. Rădulescu, L. Slătineanu, A. Munteanu, O. Dodun and G. Nagîț,

Polymers, 2022, **14**, 3061; (c) J. Wang, L. Chen, L. Zhang, C. Su and J. Feng, *Ceram. Int.*, 2022; (d) A. L. Goodwin, M. Calleja, M. J. Conterio, M. T. Dove, J. S. O. Evans, D. A. Keen, L. Peters and M. G. Tucker, *Science*, 2008, **319**, 794-797; (e) M. K. Panda, T. Runčevski, S. Chandra Sahoo, A. A. Belik, N. K. Nath, R. E. Dinnebier and P. Naumov, *Nat. Commun.*, 2014, **5**, 4811; (f) S. A. Rather, V. G. Saraswatula, D. Sharada and B. K. Saha, *New J. Chem.*, 2019, **43**, 17146-17150; (g) A. van der Lee and D. G. Dumitrescu, *Chem. Sci.*, 2021, **12**, 8537-8547; (h) H.-L. Zhou, J.-P. Zhang and X.-M. Chen, *Front. Chem.*, 2018, **6**.

2. (a) A. Bond, *Acta Crystallogr. B*, 2021, **77**, 357-364; (b) D. Das, T. Jacobs and L. J. Barbour, *Nat. Mater.*, 2010, **9**, 36-39; (c) A. Janiak, C. Esterhuysen and L. J. Barbour, *Chem. Commun.*, 2018, **54**, 3727-3730; (d) M. Kaźmierczak, E. Patyk-Kaźmierczak and A. Katrusiak, *Cryst. Growth Des.*, 2021, **21**, 2196-2204; (e) M. K. Panda, R. Centore, M. Causà, A. Tuzi, F. Borbone and P. Naumov, *Sci. Rep.*, 2016, **6**, 29610; (f) B. K. Saha, *J. Indian Inst. Sci.*, 2017, **97**, 177-191.

3. (a) J. Shen, Y. Zhao, H. Liu, Y. Niu, R. Gao, T. Guo, D. Zhao and Z. Luo, *Microgravity Sci. Technol.*, 2022, **34**, 59; (b) L. Tang and C. R. McNeill, *Macromolecules*, 2022, **55**, 7273-7283.

4. (a) A. Cuquejo-Cid, A. García-Fernández, C. Popescu, J. M. Bermúdez-García, M. A. Señarís-Rodríguez, S. Castro-García, D. Vázquez-García and M. Sánchez-Andújar, *iScience*, 2022, **25**, 104450; (b) Y.-C. Yang, X. Liu, X.-B. Deng, L.-M. Wu and L. Chen, *JACS Au*, 2022, DOI: 10.1021/jacsau.2c00353.

5. (a) V. G. Saraswatula, D. Sharada and B. K. Saha, *Cryst. Growth Des.*, 2018, **18**, 52-56; (b) A. I. Kitaigorodsky, *Molecular Crystals and Molecules*, Academic Press, 1973.

6. (a) S. Bhattacharya, V. G. Saraswatula and B. K. Saha, *Cryst. Growth Des.*, 2016, **16**, 277-284; (b) X. Ding, D. K. Unruh, R. H. Groeneman and K. M. Hutchins, *Chem. Sci.*, 2020, **11**, 7701-7707; (c) X. Ding, A. W. Crawford, W. P. Derrick, D. K. Unruh, R. H. Groeneman and K. M. Hutchins, *Chem. Eur. J.*, 2021, **27**, 16329-16333; (d) B. Dwivedi, A. Shrivastava, L. Negi and D. Das, *Cryst. Growth Des.*, 2019, **19**, 2519-2524; (e) N. Juneja, D. K. Unruh, E. Bosch, R. H. Groeneman and K. M. Hutchins, *New J. Chem.*, 2019, **43**, 18433-18436; (f) F. Marin, S. Tombolesi, T. Salzillo, O. Yaffe and L. Maini, *J. Mater. Chem. C*, 2022, **10**, 8089-8100; (g) L. Negi, S. Kumar, B. Dwivedi and D. Das, *Cryst. Growth Des.*, 2021, **21**, 1428-1433; (h) L. Negi, A. Shrivastava and D. Das, *Chem. Commun.*, 2018, **54**, 10675-10678; (i) S. A. Rather and B. K. Saha, *Cryst. Growth Des.*, 2018, **18**, 2712-2716.

7. C. B. Aakeröy and P. D. Chopade, in *Supramolecular Chemistry*, 2012, DOI: 10.1021/acs.cgd.2c00446.

8. (a) S. K. Rai, S. Allu and A. K. Nangia, *Cryst. Growth Des.*, 2020, **20**, 4512-4522; (b) M. A. Sinnwell, R. H. Groeneman, B. J. Ingenthron, C. Li and L. R. MacGillivray, *Commun. Chem.*, 2021, **4**, 60; (c) J. Vainauskas, F. Topić, O. S. Bushuyev, C. J. Barrett and T. Friščić, *Chem. Commun.*, 2020, **56**, 15145-15148.

9. K. M. Hutchins, D. K. Unruh and R. H. Groeneman, *New J. Chem.*, 2018, **42**, 16460-16463.

10. S. Khorasani, D. S. Botes, M. A. Fernandes and D. C. Levendis, *CrystEngComm*, 2015, **17**, 8933-8945.

11. M. J. Cliffe and A. L. Goodwin, *J. Appl. Crystallogr.*, 2012, **45**, 1321-1329.